ISSN 1063-7834, Physics of the Solid State, 2006, Vol. 48, No. 4, pp. 709–716. © Pleiades Publishing, Inc., 2006.
Original Russian Text © O.Z. Yanchevskiĭ, O.I. V'yunov, A.G. Belous, A.I. Tovstolytkin, V.P. Kravchik, 2006, published in Fizika Tverdogo Tela, 2006, Vol. 48, No. 4, pp. 667–673.

MAGNETISM AND FERROELECTRICITY

Synthesis and Characterization of $La_{0.7}Sr_{0.3}Mn_{1-x}Ti_xO_3$ Manganites

O. Z. Yanchevskiĭ[a], O. I. V'yunov[a], A. G. Belous[a], A. I. Tovstolytkin[b], and V. P. Kravchik[b]

[a] *Vernadskiĭ Institute of General and Inorganic Chemistry, National Academy of Sciences of Ukraine, pr. Akademika Palladina 32/34, Kiev, 03680 Ukraine*

e-mail: vyunov@ionc.kar.net

[b] *Institute for Magnetism, National Academy of Sciences of Ukraine, Kiev, 03142 Ukraine*

Received April 5, 2005

Abstract—The structural, electrical and magnetic properties of the $La_{0.7}Sr_{0.3}Mn_{1-x}Ti_xO_3$ system characterized by rhombohedral lattice distortions are studied. Substitution of titanium for manganese weakens ferromagnetism and leads to an increased resistivity. Using x-ray Rietveld full-profile refinement data and ferromagnetic resonance spectra, it is demonstrated that titanium substitution for manganese occurs with charge compensation according to the equation $Mn^{4+} \longrightarrow Ti^{4+}$ and with a simultaneous decrease in the oxygen nonstoichiometry as the value of x increases.

PACS numbers: 61.10.Nz, 76.50.+g

DOI: 10.1134/S1063783406040159

1. INTRODUCTION

The $Ln_{1-x}A_xMnO_3$ systems (where *Ln* stands for La or a rare-earth element and A^{2+} = Ca, Sr, Ba, Pb) with a perovskite structure are prominent for interrelating electrical and magnetic properties. The extreme compositions $Ln^{3+}Mn^{3+}O_3$ and $A^{2+}Mn^{4+}O_3$ are antiferromagnetic and insulating, whereas manganites $Ln_{1-x}A_xMnO_3$ exhibit coexisting ferromagnetism and metallic conductivity in the range $0.18 \le x \le 0.5$. A specific feature of the manganites with mixed oxidation of manganese ions that attracts special fundamental and practical interest is their electrical resistivity, which is strongly dependent on an external magnetic field *H* and is known as colossal magnetoresistance [1–4].

The theoretic explanation of the colossal magnetoresistance is based on the concept of double exchange, which is a continuous transfer of an electron between Mn^{3+} and Mn^{4+} ions occupying equivalent lattice sites via the 2*p* orbitals of an O^{2-} anion [5]. An important part in the magnetoresistance mechanism is played by the strong electron–phonon interaction due to the Mn^{3+} ions producing local Jahn–Teller distortions of the lattice and also by the indirect antiferromagnetic exchange [6, 7]. The latter two types of interaction counteract the ferromagnetic double exchange, thereby giving rise to quite complicated electronic and magnetic phase diagrams of the manganites.

The temperature dependences of the electric resistance $R(T)$ and magnetoresistance $MR(T)$ exhibit maxima near the temperature of transition from the ferromagnetic to paramagnetic state (the Curie temperature T_C). The magnetoresistance in the paramagnetic region is almost zero. Materials with T_C near room temperature are promising for magneto-electronic applications.

The magnetic-ordering temperature of the $Ln_{1-x}A_xMnO_3$ compounds depends mainly on the Mn^{3+}/Mn^{4+} ratio and details of the crystal structure. At present, to find methods for influencing the magnitude of magnetoresistance and the ferromagnetic–paramagnetic phase transition temperature of manganites, the effect of substitution at the *Ln* sites has been best studied. The highest temperature T_C = 375 K was obtained for the compound $La_{1-x}Sr_xMnO_3$ [8]. However, substitutions in the manganese cationic sublattice can also affect the Mn^{3+}/Mn^{4+} ratio, produce structural defects, and change the electrical and magnetic properties of manganites. The elements that do not take part in the double exchange, for example, titanium ions [9], are especially effective for this purpose.

In the $La_{0.7}Sr_{0.3}Mn_{1-x}Ti_xO_3$ system, the temperature T_C decreases to room temperature for small x, which is a prerequisite for developing practical magnetoresistance devices. Studies of titanium-doped manganites performed in [9–12] showed that increasing the titanium content leads to a significant reduction in the spontaneous magnetization and Curie temperature. However, the model of substitution of Ti^{4+} ions for Mn^{4+} ions proposed in those papers has not been confirmed by experimental studies of the structural aspects of titanium doping of $La_{0.7}Sr_{0.3}Mn_{1-x}Ti_xO_3$ [13]. Moreover, further analysis of different models is required [14, 15]. Such an analysis would only be possible based on a comprehensive study of the influence of the doping

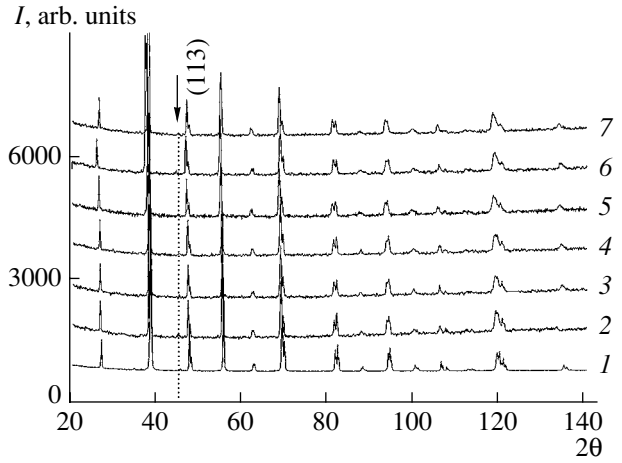

Fig. 1. X-ray diffraction patterns of $La_{0.7}Sr_{0.3}Mn_{1-x}Ti_xO_{3\pm\delta}$ samples for x equal to (*1*) 0, (*2*) 0.02, (*3*) 0.04, (*4*) 0.06, (*5*) 0.08, (*6*) 0.10, and (*7*) 0.15. The (113) superstructure peak is indicated by an arrow.

level on the structural, electrical, and magnetic properties of manganites [16].

The purpose of the present paper is to determine the charge compensation mechanism operating in titanium-doped $La_{0.7}Sr_{0.3}Mn_{1-x}Ti_xO_3$ manganites by investigating the interrelations between the structural, electrical, and magnetic properties.

2. EXPERIMENTAL TECHNIQUES

The samples for our study were produced by solid-state synthesis using reagent-grade La_2O_3, Mn_2O_3, and TiO_2 and lab-grade $SrCO_3$, which were first dried at 1120, 920, 870, and 520 K, respectively. The reagents were mixed together in quantities corresponding to the stoichiometric composition and were homogenized with the addition of distilled water in a vibration mill with corundum milling bodies for 6 h. The charge obtained was dried at 380–400 K and passed through a capron screen.

After synthesis at 1170 K for 4 h, a second homogenization by milling was performed. A homogenized powder was mixed with a coupling agent (water solution of polyvinyl alcohol) and pressed into billets 10 mm in diameter and 3-mm-thick. Ceramic samples of $La_{0.7}Sr_{0.3}Mn_{1-x}Ti_xO_{3\pm\delta}$ were sintered for 2 h at 1570–1620 K.

The contents of Mn^{3+} and Mn^{4+} in the samples were measured using iodometry (titration of iodine by a sodium thiosulfate solution). The iodine in a potassium iodide solution was substituted for by chlorine produced by dissolving a weighted manganite sample in hydrochloric acid [17]. An analysis of the crystal-chemistry side of copper substitution for manganese was performed according to the method proposed in [18] using Shannon ion radii [19].

The lattice parameters were determined using the full-profile Rietveld refinement method. X-ray diffraction measurements were performed using a DRON-4-07 diffractometer (Co$K\alpha$ radiation). Diffraction patterns were measured in a discrete mode in the range $2\theta = 10°$–$150°$ in steps $\Delta 2\theta = 0.02°$ taking 10-s expositions at each point. For an external reference, we used SiO_2 (2θ standard) and NIST SRM1979–Al_2O_3 (a certified intensity standard).

The electrical resistance of ceramic samples was measured by the four-probe method in the temperature range 77–370 K. The samples for the measurements were rectangular parallelepipeds $2 \times 3 \times 10$ mm in size. The contacts were made of silver paste and baked in. The magnetoresistance MR was measured in magnetic fields of up to $H = 1.2$ MA/m using the formula $MR = (R_0 - R_H/R_0) \times 100\%$, where R_0 is the electrical resistance in a zero field and R_H is the electrical resistance in an external magnetic field H. The magnetization was measured using an MPMS-5S SQUID magnetometer (Quantum Design). Ferromagnetic resonance was studied on $1 \times 1 \times 5$ mm samples using a RADIOPAN 9.2-GHz spectrometer. During the measurements, the magnetic field was directed along the longer side of the sample.

3. EXPERIMENTAL RESULTS

The x-ray diffraction patterns of $La_{0.7}Sr_{0.3}Mn_{1-x}Ti_xO_{3\pm\delta}$ samples obtained at room temperature are shown in Fig. 1. All samples studied are single-phase, and their crystal lattices belong to the rhombohedral system (space group $R\bar{3}c$), which is indicated by the presence of the (113) peak in the x-ray diffraction patterns. The results of the Rietveld refinement of the lattice parameters of the $La_{0.7}Sr_{0.3}Mn_{1-x}Ti_xO_{3\pm\delta}$ samples are shown in Table 1. The unit cell volume of the manganites is seen to increase as titanium is substituted for the manganese.

The temperature dependences of the electrical resistivity $\rho(T)$ of $La_{0.7}Sr_{0.3}Mn_{1-x}Ti_xO_{3\pm\delta}$ samples are shown in Fig. 2a. For samples with $x < 0.04$, the resistivity increases in the entire temperature range studied (77–370 K). Metallic conductivity is observed in the manganites only in the ferromagnetic state. The temperature T_C of the samples with $x < 0.04$ exceeds 370 K, which is in agreement with the data from [8]. For the samples with $x \geq 0.04$, the $\rho(T)$ dependences exhibit maxima within the temperature range studied, with the positions of the maxima shifting to lower temperatures with increasing x, which indicates a waning of ferromagnetism.

The temperature dependences of the magnetoresistance of $La_{0.7}Sr_{0.3}Mn_{1-x}Ti_xO_{3\pm\delta}$ samples measured in a field of 1.2 MA/m are shown in Fig. 2b. According to the published data [20–22], the magnetoresistance of single-crystal manganite samples has a maximum near

Table 1. Structural parameters of $La_{0.7}Sr_{0.3}Mn_{1-x}Ti_xO_{3\pm\delta}$

x	0	0.02	0.04	0.06	0.08	0.10	0.15
Unit cell parameters							
a, Å	5.5061(2)	5.5108(4)	5.5146(4)	5.5176(4)	5.5217(5)	5.5231(6)	5.5288(5)
c, Å	13.3616(3)	13.3674(6)	13.3743(6)	13.3801(6)	13.3806(7)	13.3887(7)	13.4005(6)
c/a	2.4258	2.4257	2.4253	2.4249	2.4232	2.4241	2.4237
V, Å^3	350.81(2)	351.57(4)	352.24(4)	352.76(4)	353.29(5)	353.69(6)	354.74(5)
Coordinates of ions							
O : x	0.464(3)	0.460(3)	0.459(3)	0.460(3)	0.458(3)	0.458(4)	0.457(5)
Reliability factors							
R_B, %	5.91	5.40	5.90	5.89	5.56	5.66	6.05
R_f, %	7.17	7.00	7.30	6.69	6.19	6.48	5.06

Note: The positions and coordinates of ions in the $R\bar{3}c$ structure are La 6*a* (0, 0, 1/4), Mn 6*b* (0, 0, 0), and O 18*e* (*x*, 0, 1/4).

the Curie point and decreases as the temperature goes away from T_C. Polycrystalline samples exhibit an additional contribution to the MR in the low-temperature region $T < T_C$; this contribution steadily grows with decreasing temperature. The additional contribution is assumed to be related to either spin-dependent scattering of the charge carriers in the intergrain regions [21] or to spin-polarized tunneling through the intergrain boundaries [22]. Both of the contributions to the magnetoresistance are clearly seen (Fig. 2b, curve *1*) in the $La_{0.7}Sr_{0.3}Mn_{1-x}Ti_xO_{3\pm\delta}$ sample without titanium (x = 0); the magnetoresistance increases near T_C ($T > 300$ K) and at low temperatures ($T < 150$ K). This kind of behavior of the MR(T) curves is preserved up to $x \sim 0.04$; as x increases further (lines *4–7*), the growth of the magnetoresistance at high temperatures becomes less and less pronounced, which is in agreement with the data from [23].

The dependences of the Curie temperature and the maximum value of the electrical resistivity of $La_{0.7}Sr_{0.3}Mn_{1-x}Ti_xO_{3\pm\delta}$ samples on the extent of titanium substitution for manganese are shown in Fig. 3a. Weakening of ferromagnetism in doped manganites is usually accompanied by a growth of the electric resistivity. In our case, this trend is also observed; namely, the increase in x in $La_{0.7}Sr_{0.3}Mn_{1-x}Ti_xO_{3\pm\delta}$ causes the electric resistivity to increase. The phase transition temperature decreases with an increase in x, and the $T_C(x)$ dependence is almost linear. The rate of the decrease in T_C with increasing x (~5 K/mol % Ti) is substantially smaller than that in germanium-doped manganites (~28 K/mol % Ge) [24], where, similar to titanium, the germanium ions have an oxidation level of 4+ and no electrons on the *d* orbitals but, in contrast to titanium, are significantly different from manganese ions in terms of their size ($R_{Mn^{4+}} = 0.53$ Å, $R_{Ti^{4+}} = 0.605$ Å, $R_{Ge^{4+}} = 0.53$ Å).

The dependences of the MR on the titanium content measured in a magnetic field of 1.2 MA/m at 77 and 295 K are shown in Fig. 3b. The MR(x) dependence at 295 K has a maximum of ~ 8% at $x = 0.08$, and the magnetoresistance of undoped $La_{0.7}Sr_{0.3}MnO_3$ is ~ 5%. The maximum value of the MR(x) at 295 K in $La_{0.7}Sr_{0.3}Mn_{1-x}Ti_xO_{3\pm\delta}$ samples is observed at $x = 0.08$ because of the shift of T_C closer to room temperature.

The ferromagnetic resonance spectra of $La_{0.7}Sr_{0.3}Mn_{1-x}Ti_xO_{3\pm\delta}$ samples measured at 77 K are shown in Fig. 4. The behavior of these spectra is typical of the ferromagnetic state of doped manganites [25, 26]; the resonance field is $B_r \cong 220$ mT, and the linewidth is $w \cong 105$ mT. It can be seen that the low-temperature magnetic state is almost independent of x up to $x = 0.15$.

4. DISCUSSION OF THE RESULTS

In order to explain the observed dependences, the experimental data are compared with theoretical calculations based on different models of charge compensation of titanium substituting for manganese. The calculations are performed under the assumption that the manganese in the manganites can take the form of Mn^{3+} and Mn^{4+}. Manganese ions with an oxidation level of 2+ (Mn^{2+}) can appear only if there are a lot of vacancies in the lanthanum sublattice [27] (vacancies in the oxygen sublattice do not create Mn^{2+} [28]). A chemical analysis of a $La_{0.7}Sr_{0.3}Mn_{1-x}Ti_xO_{3\pm\delta}$ sample with $x = 0$ shows that the deviation of the oxygen content from the stoichiometric value is $\delta = +0.035$, which is sufficiently small to exclude the Mn^{2+} ions from the consideration. Therefore, in our calculations, we assume that the oxidation level of manganese can be 3+ and 4+ and that the titanium can have oxidation levels (3+, 4+). The value of δ in $La_{0.7}Sr_{0.3}MnO_{3+\delta}$ is positive because of the cationic vacancies. Therefore, as demonstrated

in [18], we can represent this solid solution in the form $(La_{0.7}Sr_{0.3})_{1-\delta/3}V_{A,\delta/3}Mn^{3+}_{0.7-2\delta-\delta/3}Mn^{4+}_{0.3+2\delta}V_{B,\delta/3}O_3$, where V_A and V_B denote vacancies in sublattices A and B, respectively, of the complex perovskite ABO_3. In addition, from studying the temperature dependences of the Seebeck effect in strontium-doped manganites, it was concluded in [29] that the $La_{0.8}Sr_{0.2}MnO_3$ solid solution contains Mn^{3+} ions both in the high-spin (HS) and low-spin (LS) states and that their concentrations are in the ratio $Mn^{3+}_{HS} : Mn^{3+}_{LS} \approx 3 : 1$. The coexistence of Mn^{3+}_{HS} and Mn^{3+}_{LS} has been confirmed both experimentally [30] and theoretically [31]. Therefore, the strontium-doped manganites under study can be represented as

$$(La_{0.7}Sr_{0.3})_{1-\delta/3}V_{A,\delta/3}\left(\frac{3}{4}Mn^{3+}_{HS}\frac{1}{4}Mn^{3+}_{LS}\right)_{0.7-2\delta-\delta/3}Mn^{4+}_{0.3+2\delta}V_{B,\delta/3}O_3.$$

In [18], the structure data for a large number of complex oxides $A_{1-a}A'_aB_{1-b}B'_bO_{3\pm\delta}$ with a perovskite structure were analyzed and the following relation between the free unit cell volume $V_{f,s}$ and the tolerance factor t was found:

$$V_{f,s} = (1.20 \pm 0.09) - (0.95 \pm 0.09)t, \quad (1)$$

where

$$t = \frac{\langle A\text{–O}\rangle}{\sqrt{2}\langle B\text{–O}\rangle}, \quad (2)$$

$$V_{f,s} = \frac{V_{u,s} - V_{occ}}{V_{u,s}}, \quad (3)$$

$\langle A\text{–O}\rangle$ and $\langle B\text{–O}\rangle$ are the mean distances between the cations and oxygen atoms for cations A and B, respectively; $V_{u,s}$ is the experimentally measured unit cell volume; and V_{occ} is the occupied volume within the unit cell, which is equal to the sum of the volumes of all ions and vacancies calculated from the ion radii. It follows from Eqs. (1) and (3) that

$$V_{u,s} = V_{occ}/(0.95t - 0.2),$$
$$\Delta V_{u,s} = V_{occ}(0.09t - 0.09)/(0.95t - 0.2)^2. \quad (4)$$

In the calculations, we assumed that sublattice A contains cations La^{3+} (r_{La} = 1.36 Å) and Sr^{2+} (1.44 Å); sublattice B contains Mn^{3+}_{HS} (0.645 Å), Mn^{3+}_{LS} (0.72 Å), Mn^{4+} (0.53 Å), Ti^{3+} (0.67 Å), and Ti^{4+} (0.605 Å); and the anion sublattice consists of O^{2-} ions (1.36 Å). The radius of cationic vacancies for oxygen contents above the stoichiometric value ($\delta > 0$) is calculated using the equations [18]

$$r_{V,A} \approx r_A\sqrt[3]{V_{f,s}}, \quad r_{V,B} \approx r_B\sqrt[3]{V_{f,s}}. \quad (5)$$

Equations (2), (4), and (5) are employed to calculate the unit cell volumes in $La_{0.7}Sr_{0.3}Mn_{1-x}Ti_xO_{3\pm\delta}$ solid solutions when considering different mechanisms of compensation of the titanium charge in the manganese sublattice. From this point of view, we analyzed our data and the experimental results from [13, 32], where the $La_{0.7}Sr_{0.3}Mn_{1-x}Ti_xO_{3\pm\delta}$ compounds with a large titanium content were studied.

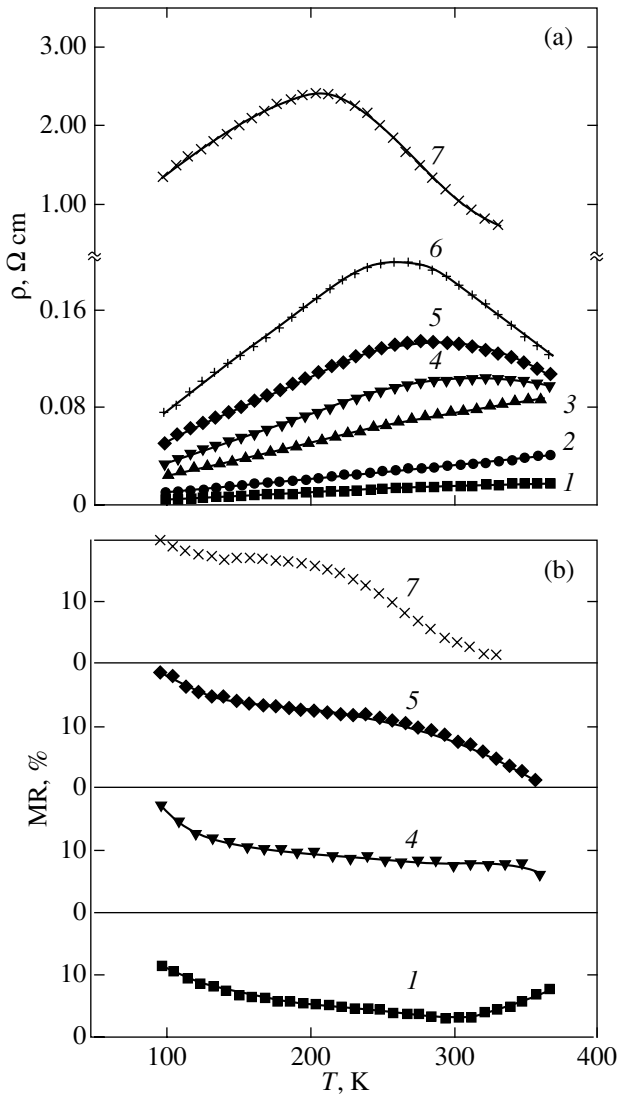

Fig. 2. Temperature dependences of (a) the electrical resistivity and (b) magnetoresistance measured at 1.2 MA/m for $La_{0.7}Sr_{0.3}Mn_{1-x}Ti_xO_{3\pm\delta}$ samples with x equal to (*1*) 0, (*2*) 0.02, (*3*) 0.04, (*4*) 0.06, (*5*) 0.08, (*6*) 0.10, and (*7*) 0.15.

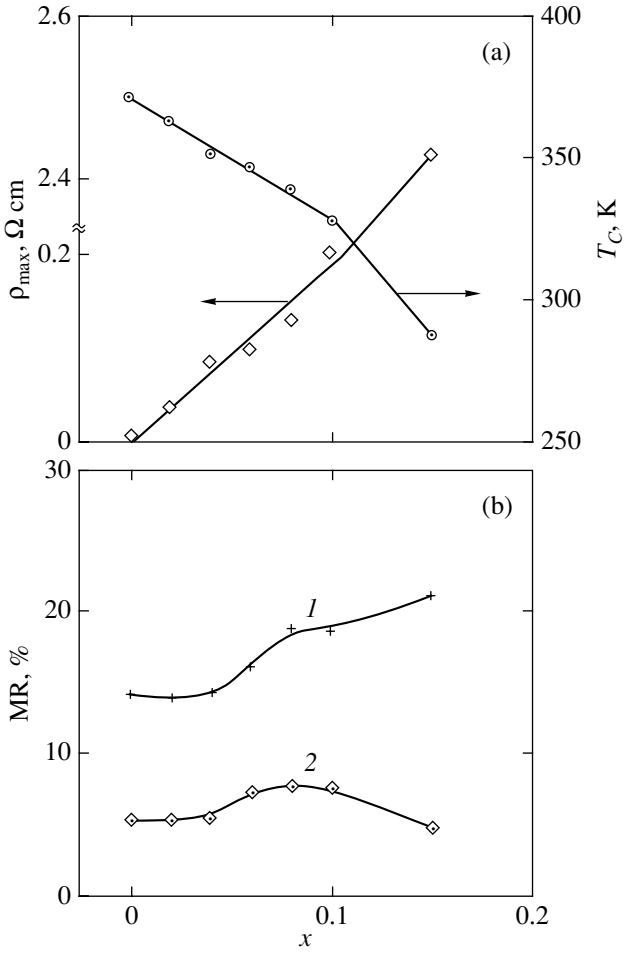

Fig. 3. Variations in (a) the Curie temperature T_C, maximum electrical resistivity ρ_{max}, and (b) magnetoresistance MR measured at (*1*) 77 and (*2*) 295 K with titanium content for $La_{0.7}Sr_{0.3}Mn_{1-x}Ti_xO_{3\pm\delta}$ samples.

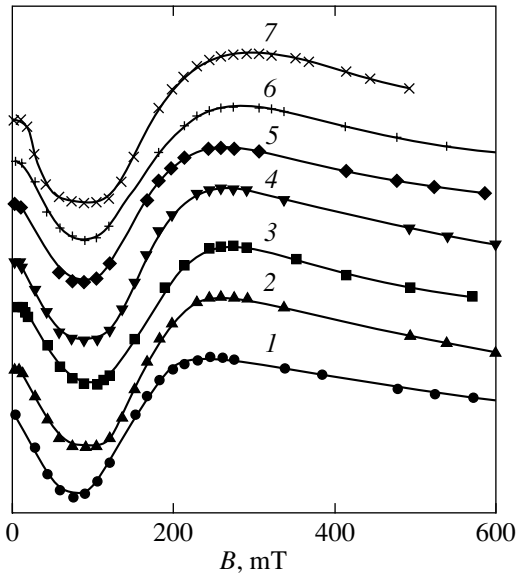

Fig. 4. Ferromagnetic resonance spectra of $La_{0.7}Sr_{0.3}Mn_{1-x}Ti_xO_{3\pm\delta}$ samples measured at 77 K for x equal to (*1*) 0, (*2*) 0.02, (*3*) 0.04, (*4*) 0.06, (*5*) 0.08, (*6*) 0.10, and (*7*) 0.15.

Figure 5 shows the dependences of the unit cell volume of the $La_{0.7}Sr_{0.3}Mn_{1-x}Ti_xO_{3\pm\delta}$ compounds on the titanium content measured experimentally and calculated using different models of the charge compensation of titanium substituted for manganese (Table 2). It can be seen from Fig. 5 that the experimental dependences cannot be described in terms of the models where the compensation of the titanium charge is assumed to occurs only in the manganese sublattice, including the $Mn^{4+} \longrightarrow Ti^{4+}$ model assumed in [11, 13]. The experimental data for $V(x)$ from [13] and the curves calculated within the $Mn^{4+} \longrightarrow Ti^{4+}$ model for $\delta = 0$ and $\delta = 0.035$ are shown in the inset to Fig. 5. For $x > 0.17$, the $V(x)$ dependence is seen to be in agreement with the calculations made within the above model for $\delta = 0$. For lower values of x, the experimental data can be fitted by the calculations only under the assumption that, simultaneously with the $Mn^{4+} \longrightarrow Ti^{4+}$ model, the oxygen

Table 2. Models of the charge compensation of titanium substituted for manganese in $La_{0.7}Sr_{0.3}Mn_{1-x}Ti_xO_{3\pm\delta}$

Model	Model of cationic vacancies in the case of excess oxygen content ($x < x_C$, $\delta > 0$)	Critical value of the Ti content* x_C ($\delta = 0$) for the initial value $\delta_0 = +0.035$	Model of anion vacancies in the case of excess cation content ($x > x_C$, $\delta < 0$)
1	$2Mn^{3+} \longrightarrow 2Ti^{4+} + (1/3)(V_A + V_B)$**		
2	$Mn^{3+} \longrightarrow Ti^{3+}$		
3	$Mn^{4+} \longrightarrow Ti^{4+}$		
4	$2Mn^{4+} \longrightarrow 2Ti^{3+} - (1/3)(V_A + V_B)$	0.070	$2Mn^{4+} \longrightarrow 2Ti^{3+} + V_O^2$
5	$(3/2)O_2 \longrightarrow ABO_3 + (V_A + V_B) + 6h$		

*As the titanium content increases, δ increases in model 1, is constant in models 2 and 3, and decreases to zero at x_C in model 4. In model 5, only intrinsic Schottky defects are taken into account; the introduced defects are not considered explicitly in this model [33].

**In calculations, the $Mn^{3+}_{HS} : Mn^{3+}_{LS}$ ratio is assumed to remain unchanged in titanium-doped manganites.

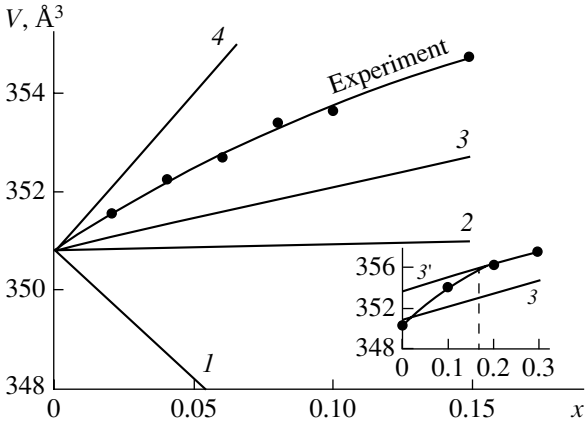

Fig. 5. Unit cell volumes of $La_{0.7}Sr_{0.3}Mn_{1-x}Ti_xO_{3\pm\delta}$ samples as a function of the titanium content x obtained from experimental data (points) and calculated (lines) for different models of the charge compensation of titanium substituted for manganese (the numerals on the lines correspond to Table 2). The inset shows the experimental data from [13] (points) and the $V(x)$ dependences calculated in the $Mn^{4+} \longrightarrow Ti^{4+}$ model for δ equal to (*3*') 0 and (*3*) 0.035.

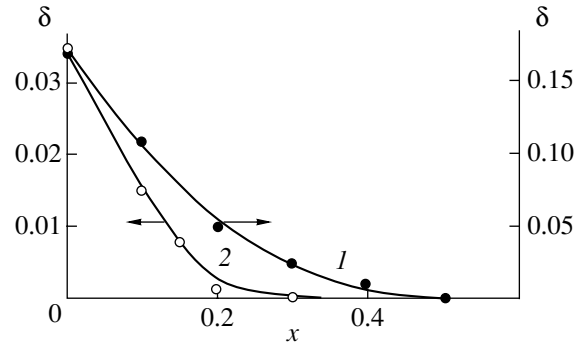

Fig. 6. Dependence of the oxygen nonstoichiometry coefficient (*1*) on the degree of substitution of strontium for lanthanum in the $La_{1-x}Sr_xMnO_{3\pm\delta}$ system according to gravimetric data from [32] and (*2*) on the degree of substitution of titanium for manganese in the $La_{0.7}Sr_{0.3}Mn_{1-x}Ti_xO_{3\pm\delta}$ system according to the structural data obtained in this study.

nonstoichiometry δ decreases as x increases. The value of δ can decrease as a result of process 4 (Table 2). However, process 4 corresponds to a different model of charge compensation and, therefore, to a different $V(x)$ dependence at $x = 0.07$, which is not supported by the experimental data (Fig. 5). Therefore, we assume that, as titanium substitutes for manganese in the $La_{0.7}Sr_{0.3}Mn_{1-x}Ti_xO_{3\pm\delta}$ compound in the range $0 \le x \le 0.17$, the number of intrinsic defects changes, as is the case in the $La_{1-x}Sr_xMnO_{3\pm\delta}$ system when strontium substitutes for lanthanum [32] (see line *1* in Fig. 6). This process is described by model 5 (Table 2), in which Schottky defects are involved [33]. The values of δ calculated in this model are shown in Fig. 6 (curve *2*). It is evident that the calculated dependence (curve *2*) agrees with the experimental data from [32] (curve *1*).

Let us consider the magnetic properties in this model of charge compensation. Figure 7a shows the dependence of the saturation magnetization M_S on the titanium content measured at 10 K in a magnetic field of 1.2 MA/m and the data from [8] obtained under similar conditions. The $M_S(x)$ dependence changes in character near $x = 0.17$; namely, at lower values of x, the saturation magnetization is weakly dependent on x, which is in agreement with the observed weak change in the ferromagnetic resonance spectra. At higher values of x, the saturation magnetization decreases much faster and almost linearly with increasing x. Figure 7a also shows the calculated $M_S(x)$ dependence for the suggested model of compensation of the titanium charge in the manganese sublattice. The calculation is performed for the following values of the magnetic moments: $Mn^{3+}_{HS} = 4\mu_B$ (spin $S = 2$), $Mn^{3+}_{LS} = 2\mu_B$ ($S = 1$), and $Mn^{4+} = 3\mu_B$ ($S = 3/2$) [34]. The observed change in the behavior of the saturation magnetization can be explained in terms of the competition of two processes at small x: one process is an increase in M_S due to the increase in δ (i.e., the increase in the number of magnetic manganese ions in the unit cell), and the other process is a decrease in M_S due to the substitution of nonmagnetic Ti^{4+} ions for magnetic Mn^{4+} ions. At high values of x, the latter process prevails and the saturation magnetization diminishes rapidly.

Figure 7b shows the dependence of the share of Mn^{4+} ions $C_{Mn^{4+}}$ in the total number of manganese ions on the titanium content. For $x = 0$, the share of Mn^{4+} is determined by chemical analysis [17], and for $x > 0$ this quantity is calculated using models 3 and 5 (Table 2). It is known [7] that the uniform ferromagnetic phase in Sr-doped manganites exists if the Mn^{4+} content is within the limits from 0.18 to 0.50 (shaded area in Fig. 7b). Outside of this range, the tendency toward antiferromagnetic ordering prevails, which gives rise to antiferromagnetism or more complex forms of magnetic ordering [7, 8]. As seen in Fig. 7b, if models 3 and 5 are valid, then the ferromagnetic state will be stable up to $x \sim 0.17$, which is in agreement with the ferromagnetic resonance data (Fig. 4). It can be expected that, in this case, as the titanium content increases, the Curie temperature will change only weakly due to the decrease in the number of magnetic ions in the immediate vicinity of the manganese ions, which is in agreement with the experimental data.

It should also be noted that, if the suggested model of compensation of the titanium charge is correct, then the behavior of the lattice and magnetic parameters observed in [13] becomes clear. It was shown in [13] that $(La,Sr)Mn_{1-x}Ti_xO_{3\pm\delta}$ manganites are ferromagnetic and that their saturation magnetization remains quite high (~$2\mu_B$ per manganese atom) up to $x = 0.3$.

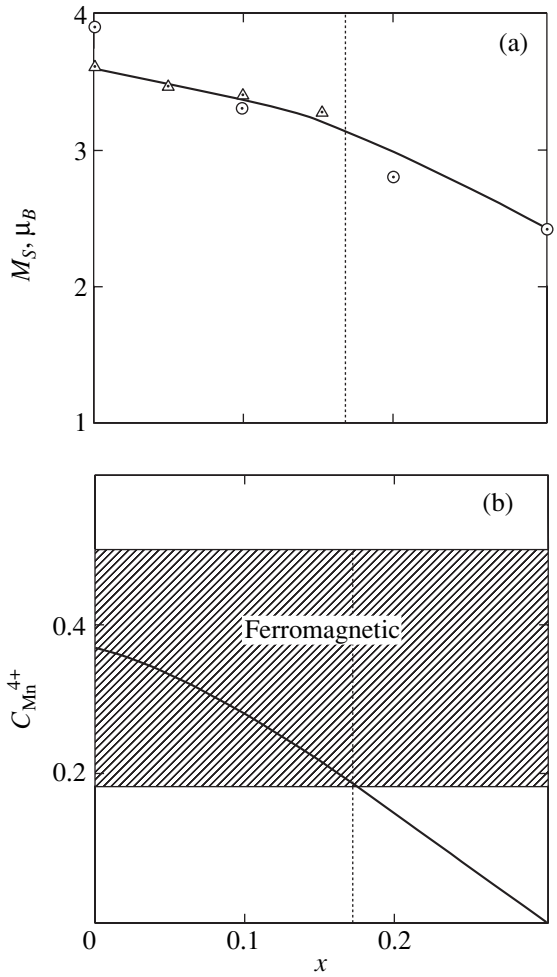

Fig. 7. (a) Calculated (solid line) and experimental dependences of the saturation magnetization in a magnetic field of 1.2 MA/m corresponding the experimental data of this work (triangles) and taken from [13] (circles). (b) The share of Mn^{4+} ions in $La_{0.7}Sr_{0.3}Mn_{1-x}Ti_xO_{3\pm\delta}$ compounds (the domain of the ferromagnetic phase is shaded).

5. CONCLUSIONS

Thus, based on the results of a comprehensive analysis of the dependences of the structural, magnetic, and resonance properties of the $La_{0.7}Sr_{0.3}Mn_{1-x}Ti_xO_{3\pm\delta}$ compounds on x, we have demonstrated that the charge compensation of titanium substituted for manganese occurs via the $Mn^{4+} \longrightarrow Ti^{4+}$ mechanism with a simultaneous decrease in the oxygen nonstoichiometry δ with increasing x. In $La_{0.7}Sr_{0.3}Mn_{1-x}Ti_xO_{3\pm\delta}$, this mechanism leads to weak variations in the magnetic properties with titanium content up to $x < 0.17$, which is in agreement with the results of our experiments and published data.

ACKNOWLEDGMENTS

This work was supported by the Ukrainian Center for Science and Technology, project no. 3178.

REFERENCES

1. R. Von Helmelt, J. Wecker, B. Holzapfel, L. Schultz, and K. Samwer, Phys. Rev. Lett. **71** (14), 2331 (1993).
2. S. Jin, T. H. Tiefel, M. McCormack, R. A. Fastnacht, R. Ramesh, and L. H. Chen, Science (Washington) **264**, 413 (1994).
3. G. Zhao, K. Conder, H. Keller, and K. A. Mueller, Nature (London) **381** (6584), 676 (1996).
4. Y. Moritomo, A. Asamitsu, H. Kuwabara, and Y. Tokura, Nature (London) **380** (6570), 141 (1996).
5. C. Zener, Phys. Rev. **82**, 403 (1951).
6. J. B. Goodenough, *Magnetism and Chemical Bond* (Interscience, New York, 1963).
7. A. J. Millis, P. B. Littlewood, and B. I. Shraiman, Phys. Rev. Lett. **74** (25), 5141 (1995).
8. A. Urushibara, Y. Moritomo, T. Arima, A. Asamitsy, G. Kido, and Y. Tokura, Phys. Rev. B: Condens. Matter **51**, 41 103 (1995).
9. I. O. Troyanchuk, M. V. Bushinsky, H. Szymczak, K. Barner, and A. Maignan, Eur. Phys. J. B **28** (1), 75 (2002).
10. J. Hu, H. Qin, J. Chen, and Z. Wang, Mater. Sci. Eng., B **90**, 146 (2002).
11. M. Sahana, K. Dörr, M. Doerr, D. Eckert, K.-H. Müller, K. Nenkov, L. Schultz, and M. S. Hegde, J. Magn. Magn. Mater. **213** (3), 253 (2002).
12. Hideki Taguchi, Masanori Sonoda, Mahiko Nagao, and Hiroyasu Kido, J. Solid State Chem. **126** (2), 235 (1996).
13. N. Kallel, G. Dezanneau, J. Dhahn, M. Oumezzine, and H. Vincent, J. Magn. Magn. Mater. **261** (1), 56 (2003).
14. B. Dabrowski, K. Rogacki, X. Xiong, P. W. Klamut, R. Dybzinski, J. Shaffer, and J. D. Jorgensen, Phys. Rev. B: Condens. Matter **58** (5), 2716 (1998).
15. Z. Bukowski, B. Dabrowski, J. Mais, P. W. Klamut, S. Kolesnik, and O. Chmaissem, J. Appl. Phys. **87** (9), 5031 (2000).
16. A. Belous, O. V'yunov, O. Yanchevskii, A. Tovstolytkin, and V. Golub, in *Proceedings of the International Conference on Electroceramics and Their Applications, Cherbourg, France, 2004* (Cherbourg, 2004).
17. L. V. Borovskikh, G. A. Mazo, and V. M. Ivanov, Vestn. Mosk. Univ., Ser. 2: Khim. **40** (6), 373 (1999).
18. H. Ullmann and N. Trofimenko, J. Alloys Compd. **316** (1), 153 (2001).
19. R. D. Shannon, Acta Crystallogr., Sect. A: Cryst. Phys., Diffr., Theor. Gen. Crystallogr. **32** (5), 751 (1976).
20. X. W. Li, A. Gupta, G. Xiao, and G. Q. Gong, Appl. Phys. Lett. **71** (8), 1124 (1997).
21. R. Gross, L. Alff, B. Büchner, B. H. Freitag, C. Höfener, J. Klein, Yafeng Lu, W. Mader, J. B. Philipp, M. S. R. Rao, P. Reutler, S. Ritter, S. Thienhaus, M. S. Uhlenbruck, and B. Wiedenhorst, J. Magn. Magn. Mater. **211** (1–3), 150 (2000).
22. K. Ghosh, S. B. Ogale, R. Ramesh, R. L. Greene, T. Venkatesan, K. M. Gapchup, R. Bathe, and S. I. Patil, Phys. Rev. B: Condens. Matter **59** (1), 533 (2000).
23. J. F. Mitchell, D. N. Argurion, C. D. Potter, D. G. Hinks, J. D. Jorgensen, and D. Bader, Phys. Rev. **54** (9), 6172 (1996).

24. J. R. Sun, G. H. Rao, B. G. Shen, and H. K. Wong, Appl. Phys. Lett. **73** (20), 2998 (1998).

25. S. Budak, M. Ozdemir, and B. Aktas, Physica B (Amsterdam) **339**, 45 (2003).

26. F. Rivadulla, L. E. Hueso, C. Jardon, C. Vazquez-Vazquez, M. A. Lopez-Quintela, J. Rivas, M. T. Causa, C. A. Ramos, and R. D. Sanchez, J. Magn. Magn. Mater. **196–197**, 470 (1999).

27. D. Abou-Ras, W. Boujelben, A. Cheikh-Rouhou, J. Pierre, J.-P. Renard, L. Reversat, and K. Shimizu, J. Magn. Magn. Mater. **233** (3), 147 (2001).

28. E. Dagotto, T. Motta, and A. Moreo, Phys. Rep. **344** (1), 1 (2001).

29. H. Kamata, Y. Yonemura, J. Mizusaki, H. Tagawa, K. Naraya, and T. Sasamoto, J. Phys. Chem. Solids **56** (7), 943 (1995).

30. B. Nadgorny, I. I. Mazin, M. Osofsky, R. J. Soulen, Jr., P. Broussard, R. M. Stroud, D. J. Singh, V. G. Harris, A. Arsenov, and Ya. Mukovskii, Phys. Rev. B: Condens. Matter **63** (57), 184 433 (2001).

31. J. M. D. Coey and S. Sanvito, J. Phys. D: Appl. Phys. **37**, 988 (2004).

32. J. Mizusaki, N. Mori, H. Takai, Y. Yonemura, H. Minamiue, H. Tagawa, M. Dokiya, H. Inaba, K. Naraya, T. Sasamoto, and T. Hashimoto, Solid State Ionics **129**, 163 (2000).

33. J. Nowotny and M. Rekas, J. Am. Ceram. Soc. **81** (1), 67 (1998).

34. A.-M. Haghiri-Cosnet and J.-P. Renard, J. Phys. D: Appl. Phys. **36**, R127 (2003).

Translated by G. Tsydynzhapov